Electron scattering from oriented holmium*

D. G. Ravenhall

Physics Department, University of Illinois, Urbana, Illinois 61801

R. L. Mercer

*Speech-Processing Group, Computer Science Department, International Business Machines Corporation,
Thomas J. Watson Research Center, Yorktown Heights, New York 10598*

Discrepancies among experiments and theory on electron scattering from oriented holmium are partially resolved. An estimate is presented which suggests that the distorted-wave Born-approximation orientation effect calculated by Wright is too large by about a factor of 2. Distorted-wave Born-approximation calculations (made with a coupled-channel program) are presented which confirm this suggestion. They agree well with the Stanford data for orientation perpendicular to the scattering plane. The previous discrepancy for orientation along the recoil-momentum direction is reduced, but is not removed. The sensitivity of these results to the charge shape is examined although a fit to the data is not made. Results are given of a complete coupled-channel calculation for the first three nuclear states. Suggestions are made for future work, and cross sections and orientation effects for energy-resolved scattering from holmium at 200 MeV are given.

> NUCLEAR REACTIONS $^{165}_{67}$Ho(e,e') oriented deformed nuclei, calculations; estimate for energy-unresolved scattering, based on elastic scattering alone; DWBA results; coupled-channel corrections; results for energy-resolved scattering, and for other orientations.

I. INTRODUCTION

There has appeared in recent years an interesting group of papers[1-9] on electron scattering from oriented holmium. In this special and experimentally very taxing application of the electron-scattering method, the orientation of the deformed $^{165}_{67}$Ho has the effect of holding the prolate nucleus along the chosen axis. Consequently, the differential cross section reveals the radial shape of the charge density along some selected radius, rather than determining the spherical average that is obtained with unaligned nuclei. The method thus provides a valuable tool for more detailed exploration of the shape of deformed nuclei accessible to the method. The outcome of the experimental and theoretical papers is unsatisfying, however, in that there are disagreements among them which preclude the drawing of definite conclusions. The purpose of the present paper is to reexamine this work, and to suggest a resolution of some of the disagreements.

In the first experimental investigation on this topic, by Safrata, McCarthy, Little, Yearian, and Hofstadter[1] (which we shall call Stan-Y), the orientation axis was the normal to the scattering plane, customarily called the Y axis, and electrons were scattered at 200 MeV over a range of angles. In the second experiment, by Uhrhane, McCarthy, and Yearian[2] (Stan-q), the orientation

axis was fixed in the scattering plane, and electrons of various energies from 160 to 460 MeV were scattered at a fixed angle which made the axis also the direction of the nuclear recoil momentum $\vec{q}$.

Theoretical investigations on this topic have been summarized by Überall.[3] We make specific reference only to work which ventures numerical values for the quantities measured in Refs. 1 and 2. The first numerical prediction was made by Penner,[4] in an unpublished Born-approximation calculation. For holmium, however, with $Z = 67$, proper inclusion of the distortion of electron wave functions by the monopole Coulomb field is essential. The first distorted-wave Born-approximation (DWBA) calculation was reported by Wright and Onley.[5] They calculated the expected effect of orientation in several directions, in anticipation of Stan-Y and experiments with other axes. Somewhat later, a similar investigation was reported by Greenstein,[6] who gave a detailed description of calculations with the Born approximation and with an approximate version[7] of DWBA. A recalculation of the Wright-Onley work, to correct a phase error, was reported by Wright[8] (W1), who also made comparison with Stan-Y. This is the first calculation of the effect which makes no approximations beyond DWBA. We show Wright's comparison of theory and experiment in Fig. 1(a). The theoretical effect of orientation is

seen to have qualitatively the same angular de-
pendence as the measured effect, but is apparently
larger by about a factor of 2. The reference Stan-
q also included a later theoretical calculation by
Wright[9] (W2). The results are shown in Fig. 1(b).
Again the theoretical effect is larger than the
experimental one, but now by a bigger factor.

Besides the theoretical-experimental discrep-
ancy in scale, which makes it difficult to use the
experiments further, there is a regularity which
all of the theoretical calculations share, but which
Stan-Y and Stan-q do not. These experiments may
be thought of as exploring, respectively, the
equatorial and the polar radial dependence of the
charge density. The assumption that the defor-
mation of holmium is predominantly quadrupole
gives the result that the changes in radius from
that of the undeformed shape, between equator and
pole, are in the ratio −1 to 2. The magnitude of
the first bump (or dip) of the alignment effect
should thus also be approximately in the ratio −1
to 2. It is to be observed from Fig. 1 that the

FIG. 1. (a) Orientation effect [Eq. (1) of text] for
orientation in the Y direction perpendicular to the scat-
tering plane for 200 MeV electrons on holmium. The
experimental points are from Stan-Y (Ref. 1) and the
curve is from Wright (Ref. 8). (b) As in (a) for electrons
scattered through 36° at various energies and orientation
along the q direction. Experimental points are Stan-q
(Ref. 2) and the curve is from Wright (Ref. 9).

theoretical curves W1 and W2 bear this ratio ap-
proximately, as do the calculations we shall re-
port, and we believe it to be a necessary result of
quadrupole deformation. [To the accuracy needed
to point up the discrepancy, the orientation effect
depends only on q (the recoil momentum), and the
horizontal scales of Figs. 1(a) and 1(b) have been
chosen to have the same q scale at small angles.]
It is evident from Figs. 1(a) and 1(b) that the ex-
perimental values for the orientation effect at
around 30° or 180 MeV depart somewhat from the
ratio −1 to 2. While it is possible that a nuclear
model of sufficient peculiarity (e.g., deformation
not of quadrupole character) could reproduce the
experimentally observed ratio $\Delta y : \Delta q$, such a
model would be in violation of the well-established
quadrupole-deformed rotational model of such
nuclei. We summarize the comparison among the
experiments Stan-Y, Stan-q, and the theories W1
and W2 as follows: W1 and W2 are consistent with
each other according to the −1 : 2 relationship but
the experiments Stan-Y and Stan-q are not; and
the experiments are not in agreement with the
theory. Our purpose in this paper is to reexplore
the theoretical part of this paradox.

The project was envisaged initially[10] as an ex-
amination of possible coupled-channel effects in
electron scattering from aligned nuclei, using
our computer program ZENITH.[11] Nuclear orienta-
tion introduces an interference of amplitudes not
encountered in the usual scattering from randomly
oriented nuclei, and thus provides a more strin-
gent test of various parts of the partial-wave anal-
ysis. It is fairly clear, however, that the dis-
crepancy between theory and experiment, of a
factor 2 at best, is much larger than can be ex-
pected from the particular dispersion effects which
a coupled-channel calculation includes, but which
a DWBA calculation omits. There are certain
other approximations and simplifications made in
Wright's calculations[5,8,9] which we avoid, but they
also do not affect the results very much. The fact
that our calculated alignment effect agrees with
Stan-Y, while W1[8] does not, is a disagreement at
the DWBA level whose origin we do not under-
stand. We shall make plausible the size of the ef-
fect we obtain by relating it to elastic scattering
from a spherically symmetric charge distribution,
thus eliminating the possibility of recoupling er-
rors that the full DWBA calculation might possess.
We shall give enough information concerning the
amplitudes and factors obtained that checks with
other calculations of this effect should be fairly
straightforward.

In Sec. II the experimental alignment effect is
defined, and the assumptions made about the tar-
get orientation are stated. The nuclear model and

its parameter values are given in Sec. III. An estimate of the expected size of the alignment effect, based only on elastic scattering by a spherically symmetric charge distribution, is presented in Sec. IV. In Sec. V we establish that the DWBA-type results of our computer program ZENITH agree with those of other programs. Some necessary properties of DWBA amplitudes are briefly recalled in Sec. VI, and are applied in Sec. VII to ZENITH amplitudes. There we present alignment-effect results and make detailed comparison with the earlier calculations. Sensitivity of the results to the particular nuclear model used and an examination of their dependence on recoil momentum at various energies are discussed in Sec. VIII. A complete coupled-channel calculation is reported in Sec. IX and compared with our DWBA results. Conclusions are summarized and future work suggested in Sec. X.

II. EXPERIMENTAL MEASUREMENT AND DEFINITION OF ALIGNMENT

The holmium nuclei are oriented by cooling the single-crystal target and imposing an external magnetic field.[1,2] The experiments do not resolve elastic electron scattering from inelastic scattering to the low-lying nuclear excited states. The quantities quoted are the differential cross section for scattering from an *unoriented* target with unresolved elastic and inelastic scattering, called $\sigma_u(E, \theta)$, and the relative effect of orientation Δ:

$$\Delta = \sigma_0(E, \theta)/\sigma_u(E, \theta) - 1, \tag{1}$$

where $\sigma_0(E, \theta)$ is the differential cross section, unresolved in energy, for the *oriented* target.

We assume with W1 that the effect of orientation, so far as a theoretical calculation is concerned, is to populate unequally the eight M levels of the spin-$\frac{7}{2}$ nucleus, where M is the component of nuclear spin along the orientation axis, but that there is no phase relationship among the M states. (In other words, the density matrix of initial nuclear spins referred to the orientation axis has elements whose magnitude depends on the target temperature and the level spacing but it is diagonal.[12]) In terms of theoretical differential cross sections $\sigma(IM \rightarrow I'M')$, where IM and $I'M'$ refer to individual initial and final nuclear states, the effect of nuclear orientation is obtained by calculating the oriented cross sections $\sigma_0^{I-I'}$ for particular levels:

$$\sigma_0(I \rightarrow I') = \sum_{M,M'} P_M \sigma_0(IM \rightarrow I'M'), \tag{2}$$

where P_M are the initial-state populations, and then the relative effect of orientation Δ for unre-

solved scattering is

$$\Delta = \sum_{I'} \sigma_0(I \rightarrow I')/\sigma_u - 1. \tag{3}$$

Here σ_u is the result corresponding to $\sum_{I'} \sigma_0(I \rightarrow I')$ for unoriented unresolved scattering, i.e., that obtained with $P_M = 1/(2I+1)$.

The method of population moments, details of which are given in Appendix A, gives insight into the manner in which the populations P_M affect Δ. The major contribution to Δ is from the $\pi = 2$ term Δ_2. This moment is directly proportional to the quadrupole part of the elastic scattering amplitude, as we discuss later, and it is revealed by the second-order nonuniformity in the M population, measured by A_2, the degree of alignment (see Appendix A). Stan-Y[1] gives A_2 as 45%. W1 quotes populations P_M which lead to $A_2 = 50.9\%$. The temperature implicit in those populations may be adjusted, while maintaining the relative spacing of the levels, so that A_2 has the value quoted in Stan-Y. The various populations are listed in Table I. While a 10% reduction in A_2 reduces the calculated Δ by about 10%, the change is not too significant, since the uncertainty in A_2 is of order $\pm 3\%$.[13]

While only a small correction, Δ_4 also contributes to the measured Δ. It reveals the presence in elastic scattering of $l = 4$ interactions, as well as $l = 2$ interactions in second order. It is thus, in principle, a different probe of the deformation of the nucleus, in the same way that $l = 4$ excitations add to our knowledge of the structure of even-even $I_g = 0$ nuclei. The coefficient R_4 is to some extent adjustable, with respect to R_2, by changing the temperature of the targets.

III. NUCLEAR MODEL FOR $^{165}_{67}$Ho

The part of the nuclear level scheme of interest here is shown in Fig. 2(a). We consider only the $K = \frac{7}{2}$ rotational band of levels built on the ground state $I = \frac{7}{2}$ and shall be mainly concerned with the levels reached from the ground state directly by (one-step) quadrupole interactions, i.e., $I = \frac{9}{2}$ and $\frac{11}{2}$. The levels are regarded as the rotational eigenstates Ψ_{KIM} of a rigid spheroid of charge $\rho(\vec{c}, z; \vec{r})$:

$$\rho(\vec{c}, z; \vec{r}) = \rho_{int}\{c[1 + \beta_{2c} Y_{20}(\Omega_{cr})], z; r\}, \tag{4}$$

where the intrinsic shape $\rho_{int}(c, z; r)$ is the Fermi type

$$\rho_{int}(c, z; r) \propto \{\exp[(r - c)/z] + 1\}^{-1}. \tag{5}$$

The Coulomb multipole potentials which effect the electron scattering are generated by the multipole moments of $\rho(\vec{c}, z; \vec{r})$:

TABLE I. Populations quoted by Wright and Onley, Refs. 5 and 8, normalized to an alignment $A_2 = 50.9\%$, and those used in the present work, normalized to the A_2 value quoted in Stan-Y (Ref. 1). For the latter values, the coefficients C_π, A_π (see Appendix A) are given for all of the orders of alignment relevant to the present work.

	Populations Refs. 5 and 8	Present work	Alignment coefficients		
M	P_M	P_M	π	R_π	A_π
$\frac{7}{2}$	0.561	0.523	0	0.354	1.000
$\frac{5}{2}$	0.254	0.259	1	0.408	0.756
$\frac{3}{2}$	0.110	0.123	2	0.242	0.448
$\frac{1}{2}$	0.046	0.056	3	0.092	0.213
$-\frac{1}{2}$	0.018	0.024	4	0.023	0.082
$-\frac{3}{2}$	0.007	0.010			
$-\frac{5}{2}$	0.003	0.004			
$-\frac{7}{2}$	0.001	0.002			

$$\rho(\vec{c}, z; \vec{r}) = \sqrt{4\pi} \sum_l \rho_l(r) Y_{l0}(\Omega_{cr}). \tag{6}$$

[We insert the factor $\sqrt{4\pi}$ so that $\rho_0(r)$ and ρ_{int} are comparable in magnitude.] For given values of c and z, the one remaining parameter β_{2c} may be determined by comparison with the strength of the quadrupole transition $I = \frac{7}{2} \to \frac{9}{2}$ measured by Coulomb excitation[15]

$$B(E2; \tfrac{7}{2} \to \tfrac{9}{2}) = 2.41 \times 10^4 \; e^2 \, \text{fm}^4. \tag{7}$$

(a)   (b)

15/2⁻ ——————— 0.499

13/2⁻ ——————— 0.345

11/2⁻ ——————— 0.210   11/2

9/2⁻ ——————— 0.095   9/2

7/2⁻ ——————— 0   7/2

$^{165}_{67}$Ho

(c)   (d)   (e)

11/2

9/2

7/2
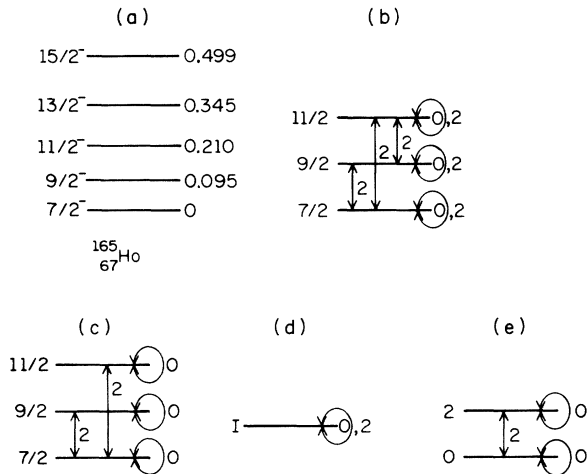
FIG. 2. (a) Nuclear level scheme for $^{165}_{67}$Ho ($K = \frac{7}{2}$ rotational band). (b), (c), (d), (e) Coupling schemes used in the coupled-channel program ZENITH (see text).

The strength is equivalent to an intrinsic quadrupole moment of $Q_0 = 7.56$ b, defined in the customary way as

$$Q_0 = 2(4\pi/5)^{1/2} \int d^3 r \, r^2 \rho(\vec{c}, z; \vec{r}) Y_{20}(\theta_{cr}). \tag{8}$$

For reasonable values of c and z, the deformation parameter β_{2c} turns out to be about 0.35, large enough that the integrals involved in inverting the expansion (6) must be performed numerically. When this is done, it turns out that there is also an appreciable hexadecapole deformation $\rho_4(r)$. The latter quantity would of course, be strongly affected by the inclusion of a deformation parameter β_{4c} in $\rho(\vec{c}, z; \vec{r})$, an additional variable we have not included in our model.[16] The theoretical DWBA calculations of Wright and Onley[5,8,9] used the small-β approximations,

$$\rho_0(r) \simeq \rho_{\text{int}}(c, z; r) \tag{9a}$$

and

$$\rho_2(r) \simeq -\beta_{2c} r [\partial \rho_{\text{int}}(c, z; r)/\partial r], \tag{9b}$$

which, as can be seen from Fig. 3, do not represent the functions accurately. (Part of this defect is accommodated in Refs. 8 and 9 by taking a rather large value for z.) Thus the determinations of c and z reported by them, from fitting σ_u and the approximate value of $Q_0 = 8$ b, are capable of improvement. Our object in the present paper is not to make a fit to the electron-scattering data, however, but rather, to repeat Wright's calculation and then, in view of the discrepancy between our result and his, to see how close to the data one comes with more recently based estimates of c and z. (The more time-consuming process of fitting will be considered at a later date.) For this estimate, there is now available information on c and z for a neighboring deformed nucleus $^{152}_{62}$Sm.[17,18] This suggests another set of parameters c and z

CHARGE DENSITY (e/fm³)

0.06

0.04 —— FULLY DEFORMED

0.02 --- SMALL-β APPROXIMATION

0

0   2   4   6   8   10

RADIUS (fm)

$^{165}_{67}$Ho

$l=0$

$l=2$
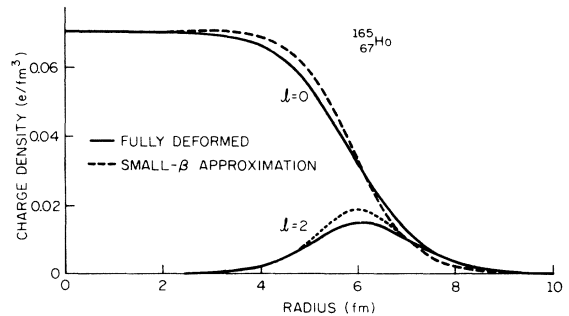
FIG. 3. Monopole and quadrupole charge distributions obtained for the shape described in Sec. III. The dashed curves are obtained by the small-β approximation [Eq. (9) of the text], the full curves by numerical calculation.

as a starting point for $^{165}_{67}$Ho, namely the samarium value of z (= 0.6014 fm), and the samarium value of c scaled up by $A^{1/3}$ (= 5.917 fm). The various sets of parameters c, z, β used by Onley and Wright, and now ours, are listed in Table II together with the Q_0 and $B(E2; \frac{7}{2} \rightarrow \frac{9}{2})$ that they yield.

We give here for completeness some well-known results concerning the rotational model.[19] An even-even nucleus with the expected level scheme of Fig. 2(d) and intrinsic quadrupole moment Q_0, has as a measure of the quadrupole transition strength

$$B(E2; 0 \rightarrow 2) = (5/16\pi)e^2 Q_0^2. \tag{10}$$

For quadrupole transitions among levels of the real $^{165}_{67}$Ho, with the level scheme of Fig. 2(b), the strength is given by

$$B(E2; I \rightarrow I') = (5/16\pi)e^2 Q_0^2 \, \gamma_{II'}^2, \tag{11a}$$

where the factor $\gamma_{II'}$ is a Clebsch-Gordan coefficient[20]

$$\gamma_{II'} = \langle IK20 | I'K \rangle. \tag{11b}$$

K is here equal to the ground-state spin $I_g = \frac{7}{2}$, and the factor $\gamma_{II'}$ is equal to 1 in the case $I = 0 \rightarrow I = 2$ ($K = 0$). A simple property of the Clebsch-Gordan coefficients produces the sum rule

$$\sum_{I'} B(E2; I \rightarrow I') = (5/16\pi)e^2 Q_0^2,$$

which for scattering in the DWBA means that the total quadrupole cross section depends only on Q_0, and not on the nuclear spins. This result was first observed by Schiff.[21]

The relationships given specify uniquely the nuclear model and the diagonal and transition multipole charge densities we shall use.

IV. ESTIMATE OF EFFECT

In this section we estimate the effect of alignment, by relating it to properties of only elastic scattering from a spherically symmetric charge distribution. The physical considerations involved give useful insight into the more general problem, and the estimate itself is accurate for the case of

small nuclear deformation, a physically uninteresting but computationally useful limit.

Our estimate is based on the following observation concerning the Born-approximation scattering from a particular quadrupole-deformed nuclear shape. To lowest order in β_{2c} the approximations (9) for the deformed charge distribution are actually equivalent to a shape somewhat different from Eq. (4), of the form

$$\rho_r(\vec{c}, z; \vec{r}) = \rho_{int}\{c, z; r[1 - \beta_{2c} Y_{20}(\Omega_{cr})]\}. \tag{12}$$

This has the property that along the direction $\vec{r}$, the radial variable is contracted by $\beta_{2c} Y_{20}(\Omega_{cr})$, so that the resulting charge profile is dilated by this factor. The Born-approximation form factor corresponding to a recoil momentum $\vec{q} = \vec{k}_i - \vec{k}_f$,

$$F(\vec{c}, \vec{q}) = (1/Ze) \int d^3 r \, e^{i\vec{q} \cdot \vec{r}} \rho_r(\vec{c}, z; \vec{r}), \tag{13}$$

depends on the relative orientation of $\vec{q}$ and $\vec{c}$, the axis of the charge distribution. If we expand it in spherical harmonics in a form similar to the expansion (6) for ρ_r:

$$F(\vec{c}, \vec{q}) = \sqrt{4\pi} \sum_l F_l(q) Y_{l0}(\Omega_{cq}), \tag{14a}$$

then the monopole and quadrupole form factors are, respectively,

$$F_0(q) = (4\pi/Ze) \int_0^\infty r^2 dr \, \rho_{r,0}(r) j_0(qr), \tag{14b}$$

$$F_2(q) = -(4\pi/Ze) \int_0^\infty r^2 dr \, \rho_{r,2}(r) j_2(qr). \tag{14c}$$

For small β_{2c}, $\rho_{r,0}$ and $\rho_{r,2}$ may be approximated by Eqs. (9). An integration by parts, and the relationship $d/dx[x^3 j_2(x)] = -x^3 j_0'(x)$, enable us to rewrite $F_2(q)$, so that in the vector recombination we can obtain

$$F(\vec{c}, \vec{q}) \simeq \frac{4\pi}{Ze} \int_0^\infty r^2 dr \, \rho_{int}(c, z; r) \tag{15a}$$

$$\times [j_0(qr) + \beta_{2c} Y_{20}(\Omega_{cq}) qr j_0'(qr)]$$

$$= [1 + \beta Y_{20}(\Omega_{cq}) q \frac{\partial}{\partial q}] F_{int}(q), \tag{15b}$$

TABLE II. Charge distribution parameter values employed in the deformed Fermi shape (see Sec. III).

Calculation	c (fm)	z (fm)	β_{2c}	Q_0 (b)	$B(E2; \frac{7}{2} \rightarrow \frac{9}{2})$ (e^2 fm^4)
Wright & Onley Ref. 5	6.18	0.57	$\cdots$	8.00	$\cdots$
Wright Refs. 8, 9	6.12	0.65	$\cdots$	8.00	$\cdots$
Present work	5.917	0.6014	0.346	7.56	2.41×10^4

where $F_{int}(q)$ is the form factor of the undeformed shape $\rho_{int}(c,z;r)$. This relationship is the expansion to first order in β_{2c}, but to *all* orders in q, of

$$F(\vec{c},\vec{q}) = F_{int}\{q[1 + \beta_{2c}Y_{20}(\Omega_{cq})]\}. \tag{16}$$

The final expression is the form factor of the shape ρ_{int} with a fixed radial dilation of magnitude $\beta_{2c}Y_{20}(\Omega_{cq})$. In other words, in Born approximation the scattering from this particular deformed shape depends only on the radial profile in the q direction, and could thus be calculated for a particular $\vec{q}$ by using the spherical shape

$$\rho_{equiv}(r) \propto \rho_{int}(c',z';r), \tag{17a}$$

$$c',z' = c,z[1 + \beta_{2c}Y_{20}(\Omega_{cq})], \tag{17b}$$

properly normalized to total charge Ze.

We wish to exploit this idea to examine holmium scattering, where the Coulomb distortion of the electron wave functions is important. A major part of the effect of Coulomb distortion can be simulated, however, by calculating Born-approximation form factors at an effective q value of the form

$$q_{eff} = q[1 + (4/3)Ze^2/cE_0]. \tag{18}$$

Clearly, this modification does not interfere with the Born-approximation relationship we have just obtained. Thus to lowest order in β_{2c}, but to all orders in q, and to some extent for all Z, we may replace electron scattering with recoil momentum $\vec{q}$ from a fixed deformed shape by scattering from a spherically symmetric shape with the same radial profile, as measured in the $\vec{q}$ direction. At this stage, we shall revert to the shape (4), preferred for analyzing experiments[15] because its skin thickness is angle independent, even though the relationships we have derived will now only hold to some further degree of approximation.

A physical nucleus, for which only the projection M of the angular momentum $\vec{I}$ along the alignment axis is controllable, presents to the incident electron a somewhat smeared-out picture of the fixed object whose scattering properties we have discussed.[22] For a classical spheroid rotating under the influence of an external (magnetic) field, $\vec{I}$ precesses about the field axis $\hat{z}$, and the symmetry axis $\hat{z}'$ of the deformation precesses about $\vec{I}$. For a static physical nucleus, defined to be the classical deformed charge rotating in only one eigenstate I,M,K of total angular momentum and momentum components along $\hat{z}$ and $\hat{z}'$, these precessions have the effect of reducing the Born-approximation quadrupole form factor by the Clebsch-Gordan coefficient factors

$\langle IM20|IM\rangle$ and $\langle IK20|IK\rangle$, respectively. (A classical time averaging of the motion produces trigonometic expressions which are approximations to these proper quantum-mechanical factors.) In the light of these extra factors, we modify the spherically symmetric shape (17) used to estimate scattering along $\vec{q}$, for a completing aligned nucleus $M = I$, by replacing (17b) with

$$c'' = c[1 + \langle II20|II\rangle\langle IK20|IK\rangle\beta_{2c}Y_{20}(\Omega_{qz})]. \tag{17c}$$

We leave the skin thickness z unchanged, in accordance with expression (4), and denote by $\sigma_{c''}$ the partial-wave cross section to be obtained with this shape. The unoriented cross section is estimated by σ_c, the partial-wave cross section obtained with $\rho_{int}(c,z;r)$. The further property of the physical holmium scattering, that of having only partial alignment to a degree A_2 (see Sec. II), involves multiplication by A_2 of the alignment effect for complete orientation, so that finally, our estimate of the observed effect is

$$\Delta = A_2(\sigma_{c''}/\sigma_c - 1). \tag{19}$$

Because of the modifications in c'' due to the nuclear motion, the estimate is justified only as a representation of the monopole-squared and the monopole-quadrupole interference terms of the physical scattering situation. It is thus to be believed only at small q values, where the quadrupole-squared terms are not important. (It could be modified to improve on this last deficiency, but an estimate of the small-q behavior is sufficient for our present purposes.)

For a general orientation direction our estimation method would be tedious, but for orientation along $\vec{q}$, $\theta_{cq} = 0$, while for orientation perpendicular to the scattering plane, $\theta_{cq} = \frac{1}{2}\pi$ for all $\vec{q}$. Thus in both of these cases, one partial-wave calculation with a spherically symmetric ρ_{equiv} of appropriately chosen radius is all that is needed. The well-known dependence of the small-q cross section on the charge radius, that a smaller radius results in a less rapidly falling cross section, then allows us to predict from Eq. (19) that Δ_y will be positive at small q. Thus simple considerations of this kind would have given an immediate indication of an error in the results of Ref. 5. The same argument relates $\Delta_y : \Delta_q$ to the relative changes in radius at the equator and the poles of the deformed shape, and thus provides a physical explanation of the $-1:2$ ratio of these quantities. This ratio is obtained by all calculations, but not by the experiments.[1,2]

It is a simple matter to apply the method to holmium. To obtain the values of c'' according to Eq. (17) we use the nuclear model parameters contained in the third row of Table II. The polar

and equatorial half radii of $\rho(\vec{r})$ in this case are different from the undeformed values by 22% and −11%, respectively. For physical holmium in the $M = I$ state, these values are reduced by the Clebsch-Gordan factors of Eq. (17c) to 10.2% and −5.1%. Thus for orientation in the Y direction, the cross section $\sigma_{\sigma''}$ of Eq. (19) is a one-channel zero-spin partial-wave cross section for 200 MeV electrons on a Fermi shape with a half radius c'' decreased by 5.1% from the value given in Table II, and with unchanged skin thickness. Plotted in Fig. 4 is the resulting Δ_y obtained from Eq. (19) with the experimental value $A_2 = 0.45$, and also the corresponding result for orientation in the q direction. The crudeness of the estimate excuses the fact that Δ_q is obtained at 200 MeV and then is plotted as a function of energy, at $\theta = 36°$, under the assumption of dependence only on the effective wave number q_{eff} (a procedure discussed in detail in Sec. VIII). In the figure we show also Wright's results.[8,9]

When we bear in mind that the validity of the estimate is limited to q values small enough that the quadrupole-squared term is unimportant [which from Fig. 5 correspond to $\theta \lesssim 20°$], the comparison suggests that the results on Ref. 8 are too large in this q range by about a factor 2. Nothing definite can be deduced at larger q from this compar-

ison, however. As a check on the estimation method itself, we have also repeated the above calculation for the case where β_{2c} is reduced by a factor $\sqrt{10}$. At 30° and 200 MeV we obtain $\Delta_q = -2.67\%$. The DWBA method described in the next sections gives the value −2.64%. Thus, under conditions needed to justify it (small q and small β) the estimate is reliable. It is also very useful as a simple intuitive picture of the scattering process.
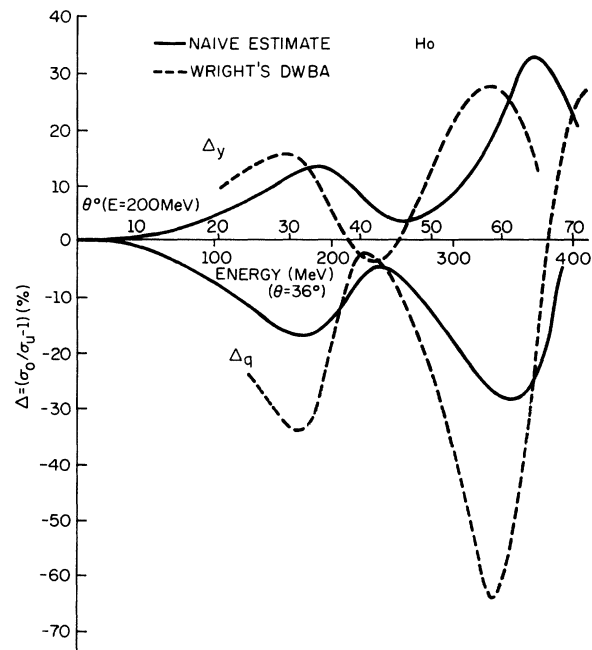
V. COMPARISON OF ZENITH WITH OTHER PROGRAMS

The heart of our method is the coupled-channel program ZENITH. Its structure and mode of operation are discussed elsewhere.[11,23] Basically it functions in the same manner as a single-channel program for elastic electron scattering, except that for each value of the total angular momentum there is a separate channel for each allowable combination of electron and nucleus angular momentum, as described in Appendix B. The number of the coupled channels is thus, for large electron angular momentum, just $N_e = \sum_n (2I_n + 1)$ where I_n is the spin of the nth nuclear state. The elastic and inelastic differential cross sections are obtained by appropriately combining the asymptotic parts of the channel wave functions. Except for numerical uncertainties, the cross sections include the effect to all orders of the inserted couplings between nuclear states. The method is thus quite different in operation and more inclusive in scope than the distorted-wave Born approximation. The latter as customarily used includes only one non-monopole coupling, between the ground state and one excited state, and calculates the inelastic cross section due to the coupling in lowest order only. Nonetheless, the difference in results between the two methods amounts in practice to a relatively small correction. Since our results are in disagreement with those of Wright, who used the version of DWBA contained in the Duke program,[24] it is incumbent on us to show first of all that under appropriate conditions our program ZENITH is in essential agreement with the Duke program. We also make comparison with the DWBA program HEINEL.[25]

We use for comparison the $l = 2$ amplitude obtained in holmium at 200 MeV, the energy of the experiment Stan-Y. For ease of definition the quadrupole transition charge density is taken to be the small-β shape, Eq. (9b), associated with the monopole Fermi shape, Eq. (5), with $c = 5.917$ fm, $z = 0.6014$ fm. The quadrupole strength used corresponds to $Q_0 = 7.56$ b. These are the parameters of the third row of Table II. The ZENITH

FIG. 4. Orientation effect [Eq. (1)] for electrons on holmium nuclei oriented in the Y and q directions. The dashed curves are those of Wright (see caption to Fig. 1) and the full curves are from the estimate of Sec. IV.

coupling scheme is that of Fig. 2(e), and all calcu-
lations assume zero excitation energy and zero
electron mass. No transverse electric or magne-
tic multipoles are included. Other values needed
to specify the calculations completely are listed
in the captions to Table III, where we list some
differential cross sections obtained from the three
programs.

The accuracy of the present ZENITH calculations
is limited by the number of terms we can include
in the Legendre series for the inelastic ampli-
tude. The coupled Dirac equations are solved up
to total angular momentum $F = \frac{69}{2}$, which for cou-
pling with the spin $I' = 2$ of the nuclear excited
state includes completely electron angular mo-
menta up to $l = 32$. The uncertainty quoted is esti-
mated from the behavior of the inelastic cross
section as this limit is varied. There is not a
corresponding uncertainty of this magnitude in
the elastic cross section since the elastic phase
shifts may be supplemented by the known point
Coulomb phase shifts. (In a new version of
ZENITH nearing completion, this present limit will
be extended considerably.) The HEINEL cross
sections in Table III are the limiting value ob-
tained by varying the number of partial waves up
to a maximum of 40 at which value there is no
further variation in the digits quoted. The Duke
code quotes cross sections and errors. They are
calculated for 40 partial waves, and the errors
quoted are so small that they do not affect the
digits we give. The close agreement among the
three inelastic cross sections listed in Table III
supports our belief that differences in results for
oriented nuclei between us and Wright[8] cannot be
due to differences in physical input, or in numer-
ical accuracy between ZENITH and the Duke code.
Compared with the unoriented cross sections of

this section, however, the amplitude recouplings
involved in Δ afford many opportunities for error,
most of which we have experienced during the
process of arriving at our present results.

As the two columns of elastic cross sections in
Table III show, ZENITH's results may differ from
other calculations (in this case, one-channel
partial-wave results) when couplings to other
channels are important. The column labeled R_{el}
gives the percentage effect. The column labeled
$R_{0+\to2+}$ gives an estimate of the corresponding ef-
fect for the inelastic scattering. It is seen that
for the coupling scheme used in this comparison,
with no diagonal quadrupole potentials, the chan-
nel couplings do not affect the *inelastic* cross sec-
tion to the accuracy we report it here. Thus they
do not interfere with the comparison we make with
the DWBA calculations.

VI. DEPENDENCE OF DWBA AMPLITUDES ON NUCLEAR SPIN

As a preliminary to our use of ZENITH amplitudes
to calculate the alignment effect, we recall some
properties of DWBA amplitudes.

The DWBA amplitude relevant to an excitation
of multipolarity l may be written

$$f^{m_s M; m'_s M'}(\theta\varphi) = \sum_m \int d^3x_e \psi_{k',m'_s}^{(-)*}(x_e) Y_{lm}^*(\Omega_e) \psi_{k,m_s}^{(+)}(x_e)$$

$$\times \int d^3x_1 \cdots x_A \Psi_{I'M'}^*(x_1 \cdots x_A)$$

$$\times \sum_{i=1}^{A} V_{lm}^{(i)}(x_i, r_e)$$

$$\times \Psi_{IM}(x_1 \cdots x_A).$$

$$(20)$$

TABLE III. Values obtained for monopole and quadrupole differential cross sections from the Duke code (Ref. 24),
the program HEINEL (Ref. 25), and the coupled-channel program ZENITH, in fm²/sr. The nuclear model is the deformed
Fermi shape, Eqs. (4) and (5) of the text, treated in the small-β approximation, Eqs. (9), and using the parameter val-
ues contained in the third line of Table II. From various ZENITH runs, the coupled-channel corrections to elastic poten-
tial scattering R_{el} and to DWBA, $R_{0+\to2+}$, are also given (see Sec. VII).

$\theta°$	HEINEL DWBA	Duke DWBA	ZENITH inelastic two channels	$R_{0+\to2+}$ (%)	ZENITH elastic two channels	ZENITH elastic one channel	R_{el} (%)
15	5.00(−1)	4.99(−1)	4.99 ± 0.02(−1)	−0.03	1.3216(2)	1.3216(2)	−0.0
30	8.44(−2)	8.44(−2)	8.42 ± 0.03(−2)	−0.05	9.976(−1)	1.0006(0)	−0.3
45	2.59(−3)	2.59(−3)	2.58 ± 0.01(−3)	−0.06	2.966(−2)	2.932(−2)	1.1
60	7.03(−4)	7.02(−4)	7.00 ± 0.03(−4)	−0.08	1.898(−3)	1.870(−3)	1.4
75	6.32(−5)	6.33(−5)	6.32 ± 0.03(−5)	−0.13	1.142(−4)	1.144(−4)	−0.2
90	1.165(−5)	1.163(−5)	1.154± 0.007(−5)	−0.02	3.277(−5)	3.193(−5)	2.6
105	5.16(−6)	5.15(−6)	5.16 ± 0.02(−6)	−0.12	1.325(−6)	1.366(−6)	−3.8
120	3.28(−6)	3.24(−6)	3.36 ± 0.02(−6)	−0.19	7.739(−7)	7.708(−7)	0.4

The functions ψ are positive-energy Dirac spinors for the incoming and outgoing electrons, properly distorted (from their plane-wave parts) by the monopole interactions with the charge distribution of the initial and final nuclear states I and I'. The subscripts m_s, m_s' on ψ indicate the spin-directions of the upper components in the asymptotic part of the wave, far from the scattering center. The Ψ are Schrödinger A-body wave functions for the nucleus. The magnetic quantum numbers all refer to some fixed axis, as yet unspecified. We are not concerned here with the dependence of f on θ, φ, the electron-scattering angle, but only on the nuclear-*spin* coordinates I, M, I', M', on the electron spins m_s, m_s', and on the direction in space of the quantization axis. The Wigner-Eckart theorem applied to the nuclear matrix element gives for its entire dependence on nuclear spins the Clebsch-Gordan coefficient expression $\langle IMlm | I'M' \rangle / (2I'+1)^{1/2}$, where the square root factor is needed because of time reversal invariance. This dependence is an automatic consequence of the DWBA assumption, but for our amplitudes, obtained by a quite different calculational procedure, it is a useful check on our methods. Moreover, it allows us to approximate $I = \frac{7}{2}$ calculations by others of smaller dimensionality.

ZENITH uses a partial-wave approach in which the chosen axis is that of the incoming electron, not a direction of interest for comparison with the present experiments. The amplitudes $f^{m_s, M; m_s', M'}$ which it produces, as described briefly in Appendix B, are to be used only in the combination

$$\rho(MM'', M'M''') \propto \frac{1}{2} \sum_{m_s m_s'} f^{m_s M, m_s' M'}(\theta\varphi)^* f^{m_s M'', m_s' M'''}(\theta\varphi),$$

(21)

which is the nuclear-spin density matrix. ρ is normalized to have unit trace, as usual, and it involves averaging and summing over initial and final electron spins, since the electron spin is not observed. To obtain the amplitudes and the nuclear-spin density matrix corresponding to some other direction of quantization—the alignment axis of interest—it is a simple matter to superpose the f amplitudes with the appropriate D functions[20] for rotation of the nuclear-spin axis:

$$f^{m_s, M_r; m_s' M_r'}_{\text{rot}} = \sum_{MM'} D^{(I)*}_{MM_r}(\vec{\omega}) f^{m_s, M; m_s' M'} D^{(I')}_{M'M_r'}(\vec{\omega}).$$

(22)

The rotated density matrix $\rho_{\text{rot}}(M_r M_r''; M_r' M_r''')$ is obtained immediately by using Eq. (21). Since the electron spins are all summed over in ρ_{rot}, it is a simple matter of completeness to show that the

electron spins do not need to be rotated.

In these arguments we are concerned only with rotations in one frame of reference—the center-of-momentum frame—and do not use Lorentz transformations. These considerations are thus formally the same as for nonrelativistic incident particles. The relativistic nature of the problem is built into the calculation of the amplitudes f in a basic way, of course. It affects the DWBA expression, Eq. (20), in the manner in which the electron matrix element is evaluated, in that the appropriate small-component parts of ψ must be included. The dependence on electron spin is simple. Without any approximation, the general amplitudes for this process, with the beam direction as quantization axis, satisfy the parity relationship expressed in Eq. (B6a) of Appendix B. We can obtain the $m_s = -\frac{1}{2}$ amplitude from the $m_s = \frac{1}{2}$ amplitude by using this symmetry. All calculations we report here were made, for speed and simplicity, under the approximation of zero electron mass. The resulting helicity conservation property of the electrons means that the Z-direction electron spin-flip amplitude $f^{1/2M; -1/2M'}$ is simply related to the nonflip amplitude $f^{1/2M; 1/2M'}$ according to Eq. (B6b). There is thus essentially only one independent electron-spin amplitude, $\frac{1}{2} \to \frac{1}{2}$.

VII. DWBA CALCULATION

The ZENITH calculation of Sec. V provides us not only with inelastic cross sections, but with an alternative way to obtain DWBA monopole and quadrupole scattering amplitudes. There are higher-order effects in the ZENITH amplitudes, indicated by the quantities R_{el} and R_{0+-2+} in Table III, but they are small. We therefore use the ZENITH amplitudes to make a calculation of the alignment effect equivalent in scope to the DWBA calculations of Wright and Onley.[5,8,9]

Referring to Sec. V and Appendix B we use ZENITH with the coupling scheme of Fig. 2(e). The Coulomb monopole potentials $\varphi_0^{11}(r) = \varphi_0^{22}(r)$ of Eq. (B4), generated by some charge density $\rho_0(r)$, are the only interaction diagonal in the nuclear states. The Coulomb quadrupole potential $\varphi_2^{12}(r)$, due to a charge density $\rho_2(r)$ normalized to the intrinsic quadrupole moment Q_0, is used to couple the 0+ and 2+ states (with no diagonal quadrupole interaction in the 2+ state). The arguments of Sec. VI allow us to extract monopole and quadrupole amplitudes $\mathcal{C}_\mu^\lambda$, $\lambda = 0, 2$, from the ZENITH amplitudes $f^{IM; I'M'}$ (we suppress the inessential electron spin indices, and insert instead the spin value of the nuclear state) according to the relationship

$$f^{IM; I'M'}(\theta) = \sum_{\lambda \mu} \mathcal{C}_\mu^\lambda(\theta) \langle IM\lambda\mu | I'M' \rangle (2I'+1)^{-1/2}. \quad (23a)$$

From the elastic scattering amplitude, $I = I' = 0$, we obtain

$$f^{0,0;0,0}(\theta) = \mathcal{Q}^0(\theta),\tag{23b}$$

and from the inelastic amplitude, $I = 0$, $I' = 2$,

$$f^{0,0;2,M'}(\theta) = \mathcal{Q}_\mu{}^2(\theta)/\sqrt{5}\,\delta_{M'\mu}.\tag{23c}$$

A rotation from the beam (z) axis may be carried out as explained in Sec. VI, so that the magnetic quantum number μ may be taken to refer to the chosen alignment axis. The DWBA-like amplitudes $g^{IM;I'M'}(\theta)$ for physical holmium, calculated according to the coupling scheme of Fig. 2(c), and including the factors γ_{II} contained in Eq. (11), are then given by

$$g^{IM;I'M'}(\theta) = \mathcal{Q}^0(\theta)\langle IM00|I'M'\rangle + \mathcal{Q}_\mu{}^2(\theta)\gamma_{II'}\langle IM2\mu|I'M'\rangle.\tag{24}$$

The orientation moments of the differential cross sections for the aligned nucleus $\sigma_\tau^{I\text{-}I'}$, as defined in Appendix A, are

$$\sigma_\tau^{I\text{-}I'}(\theta) = \sum_{MM'}(-1)^{I-M}\langle IMI-M|\pi 0\rangle|g^{IM;I'M'}(\theta)|^2.\tag{25}$$

The quantity $\sigma_0^{I\text{-}I'}(\theta)$ is just $(2I+1)^{1/2}$ times the unpolarized cross section for the indicated transition, so it follow very simply that σ_u, the unpolarized unresolved cross section, is given by

$$\sigma_u(\theta) = \sum_{I'}R_0\sigma_0^{I\text{-}I'} = |\mathcal{Q}^0|^2 + \frac{1}{5}\sum_\mu|\mathcal{Q}_\mu{}^2|^2.\tag{26}$$

The disappearance of I in this expression is a result of the Schiff sum rule for rotational excitation.[21] The general moment $\sigma_\tau^{I\text{-}I'}$ is easy to calculate. It is

$$\sigma_\tau^{I\text{-}I'}(\theta) = \sum_{\lambda\mu\lambda'\mu'}(-1)^{\tau+2I+\mu'}\mathcal{Q}_\mu^\lambda(\theta)^*\mathcal{Q}_{\mu'}^{\lambda'}\begin{Bmatrix}2 & I & I\\I' & \lambda' & \lambda\end{Bmatrix}$$

$$\times\langle\lambda-\mu\lambda'\mu'|\pi 0\rangle\gamma_{II'}(\lambda)\gamma_{II'}(\lambda'),\tag{27}$$

where $\lambda\mu$ and $\lambda'\mu'$ run over $\lambda=\mu=0$ (monopole) and $\lambda=2$, $-2<\mu<2$ (quadrupole), and $\{\cdots\}$ is a six-j symbol.[20] We also indicate by $\gamma_{II'}(\lambda)$ either $\gamma_{II'}$ ($\lambda=2$) or 1 ($\lambda=0$). The order π of the moment is restricted to $\pi=0,2,4$ by the Clebsch-Gordan coefficient. For clarity we expand this sum for the case $\pi=2$, the dominant term:

$$\sigma_2^{I\text{-}I'}(\theta) = 2/[5(2I+1)]^{1/2}\mathrm{Re}(\mathcal{Q}^{0*}\mathcal{Q}_0{}^2)\gamma_{II'}\delta_{II'}$$

$$-(-1)^{I+I'}(|\mathcal{Q}_0{}^2|^2 - |\mathcal{Q}_{-2}{}^2|^2 - |\mathcal{Q}_2{}^2|^2 + \tfrac{1}{2}|\mathcal{Q}_{-1}{}^2|^2 + \tfrac{1}{2}|\mathcal{Q}_1{}^2|^2)(\tfrac{2}{7})^{1/2}\begin{Bmatrix}2 & 2 & 2\\I' & I & I\end{Bmatrix}\gamma_{II'}{}^2.\tag{28}$$

The unresolved cross section for oriented holmium σ_0, as given by the $\lambda=2$ moment, simplifies to become

$$\sigma_0(\theta) \simeq \sum_{\substack{I'\\\tau=0,2}}R_\tau\sigma_\tau^{I\text{-}I'}(\theta)$$

$$= \sigma_u + R_2\{2/[5(2I+1)]^{1/2}\mathrm{Re}(\mathcal{Q}^{0*}\mathcal{Q}_0{}^2)$$

$$+ 2/[7\sqrt{5}(2I+1)^{1/2}](|\mathcal{Q}_0{}^2|^2 - |\mathcal{Q}_{-2}{}^2|^2 - |\mathcal{Q}_2{}^2|^2 + \tfrac{1}{2}|\mathcal{Q}_1{}^2|^2 + \tfrac{1}{2}|\mathcal{Q}_{-1}{}^2|^2)\}\langle II20|II\rangle\tag{29}$$

from which we may calculate Δ immediately.

At this stage we may compare the interference term with the results of the estimate of Sec. IV, so far as the inclusion of all the proper factors is concerned. For this purpose it is sufficient to consider the Born-approximation limit. The average over alignments of the Born-approximation cross sections of Sec. IV, Eqs. (14), is easily shown to be

$$\sigma_{u,\text{Born}} = \sigma_{\text{Mott}}\{[F_0(q)]^2 + [F_2(q)]^2\}.\tag{30}$$

By comparison with Eq. (26), it is then clear that in the Born limit, $\mathcal{Q}^0 \to \sigma_{\text{Mott}}{}^{1/2}F_0(q)$ and, for orientation in the q direction, $\mathcal{Q}_\mu{}^2 \to \sqrt{5}\,\sigma_{\text{Mott}}{}^{1/2}F_2(q)\delta_{\mu 0}$. If Eq. (A4) is used to replace R_2 by A_2, the actual

degree of alignment, we obtain, up to the monopole-quadrupole interference term in Eq. (29),

$$\sigma_{0,\text{Born}} \simeq \sigma_{u,\text{Born}} + \sigma_{\text{Mott}}A_22\sqrt{5}\,F_0(q)F_2(q)(\langle II20|II\rangle)^2$$

$$\simeq \sigma_{\text{Mott}}[F_0(q) + A_2\sqrt{5}\,F_2(q)(\langle II20|II\rangle)^2]^2.\tag{31}$$

This result says that for orientation in the q direction, the effective form factor is just $F_0(q) + A_2\sqrt{5}\,F_2(q)(\langle II20|II\rangle)^2$. The extra factors in the quadruple term compared to the argument of Sec. IV, Eqs. (14), are all immediately identifiable as proper to the scattering from physical holmium. One Clebsch-Gordan coefficient comes from the quantum-mechanical smearing due to rotation of I about the alignment axis. The other is the re-

duced matrix element associated with elastic scat-
tering. The factor A_2 is the actual degree of
alignment. The factor $\sqrt{5}$ comes from the ratio
of $Y_{20}(0)$ and Y_{00}. By this comparison, we believe
Eq. (29) to contain the correct numerical factors.

ZENITH amplitudes f obtained using the coupling
scheme of Fig. 2(e), such as those described in
Sec. V [Eqs. (33b) and (33c)] give us monopole and
quadrupole amplitudes $\mathcal{C}^0$, $\mathcal{C}_\mu{}^2$. A superposition
of the $\mathcal{C}$'s is obtained from the quite different
scheme of Fig. 2(d) with $I \geq 1$, from which the
separate values of $\mathcal{C}^0$, $\mathcal{C}_\lambda{}^2$ may be obtained by the
inverse relationship to Eq. (23a). The agreement
among the different sets of $\mathcal{C}$ so obtained (to an
accuracy limited by small higher-order effects)
demonstrates an internal consistency which checks
the algebra of our physical input. The agreement
with DWBA codes documented in Sec. V checks
the overall scale of the quadrupole effects. The
phase choices associated with the f amplitudes are
checked by the fact that when the nucleus is sub-
jected to rotations according to Eq. (22), the
cross section of Eq. (29) exhibits the angular de-
pendence expected from Sec. IV. These, and the
checks on the physical factors contained in Eq.
(31), leave no possibility for ambiguity or error
that we are aware of.

We are now at the stage where we can repeat
Wright's calculations.[8,9] The model used is the
small-β approximation to the nuclear model of
Sec. III, as contained in Eqs. (9). The parameter
values are those contained in the second line of
Table II, with an alignment factor $A_2 = 0.509$. For
scattering from holmium at 200 MeV, the mono-
pole and total quadrupole cross sections nor-
malized to $Q_0 = 8.0$ b are shown in Fig. 5. Their
sum, the unresolved unoriented cross section σ_u,
is also given, and compared with the Stan-Y data.[1]
The agreement with Fig. 1 of Ref. 8 is complete,
as we expect from the agreement in Table III. The
orientation effect we obtain for these parameter
values is shown in Fig. 6, and is compared with
the results reported in Ref. 8. There is consider-
able difference between the two curves. The dis-
crepancy is about a factor 2 around $\theta = 30°$, but in
detail, the curves cannot be reconciled by any
such simple manipulation as multiplication by a
constant factor.

We do not believe that there are any significant
errors due to numerical procedures in our result.
We have examined, of course, the effect on Δ of
the error quoted in Table III in our ZENITH calcu-
lations. It is associated with a necessary trunca-
tion of the Legendre series, and after calculating
Δ for various limits on the series, we find an ef-
fect too small to show on the graph. The possible
contributions due to higher-order effects in our
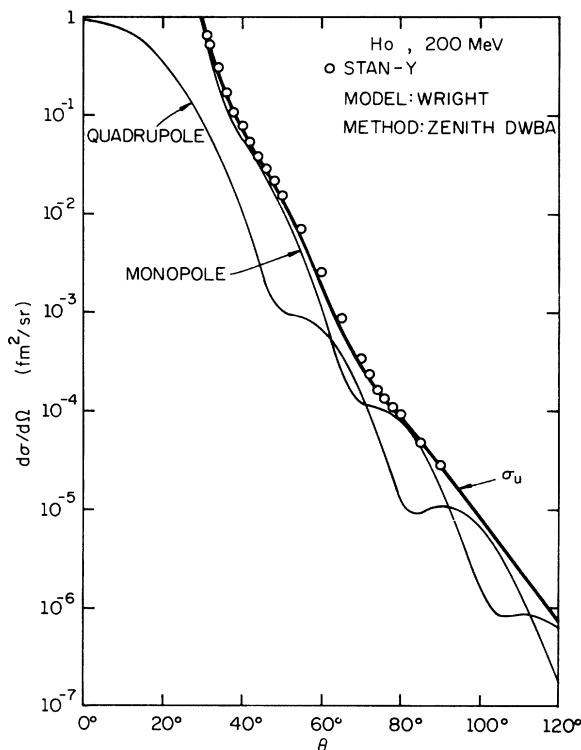
FIG. 5. Differential cross section and its monopole
and quadrupole components for 200 MeV electrons on
unoriented holmium. The nuclear model is that em-
ployed by Wright (see Sec. III). The calculational meth-
od uses the DWBA method described in Sec. VII.

DWBA-like amplitudes, mentioned at the beginning
of this section, are not negligible. The coupled-
channel calculation described in Sec. IX contains
more fully the higher-order effects associated with
the rotational levels, however, and they are very
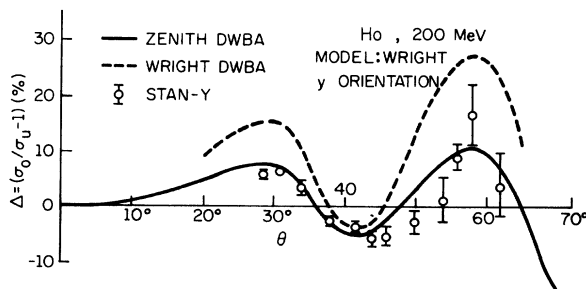
FIG. 6. Orientation effect for 200 MeV electrons on
holmium nuclei oriented in the Y direction. The nuclear
model is that employed by Wright (see Sec. III). The
dashed curve is that of Wright (Ref. 8) and the full curve
is the present version of the same calculation as ob-
tained according to Sec. VII.

small compared with the difference exhibited in Fig. 6.

This discrepancy between the present results and the DWBA calculation of Wright and Onley[5,8] is not, we believe, due to differences in physical input or assumptions, or in the published formulas.[5,8] Their expression for the DWBA quadrupole amplitude, Eq. (6) of Ref. 5, appears to contain the same dependence on nuclear spin I and I' as does our amplitude Eq. (24), apart from the phase factor noted in Ref. 8. The comparison of ZENITH and DWBA inelastic cross sections contained in Table III, made for the case $I = 0 \rightarrow I' = 2$ which involves the full quadrupole strength of Q_0, shows that for unoriented nuclei our calculational schemes produce identical answers. This verifies the proper scale of our quadrupole effects. It therefore appears that formally the method described in this section should parallel, and agree with, that of these authors. We do not know why they do not, but we believe our results to be correct.

Our numerical results may be reconciled with those obtained using the plane-wave Born approximation. Figures illustrating Born-approximation calculations appear in a number of the papers cited, and they originate from Greenstein's article.[6] Translated into our notation, Greenstein's expression for the oriented cross section agrees exactly with what we give here. With the simple shapes used in those calculations $[\rho_0(r) \propto \theta(R - r), \rho_2(r) \propto \delta(r - R)]$, we obtain an orientation effect A_y in complete agreement with that given in Fig. 3 of Stan-Y.[1] To make a further comment, we show both A_y and σ_u in Fig. 7. The first maximum of A_y occurs at about $\theta = 33°$, where $A_y \simeq 19\%$. In this angular range the monopole part of the Born approximation σ_u has a diffraction zero at $\theta \simeq 40°$ which is only partially filled in by the quadrupole scattering. On physical grounds it is to be expected that any significant improvement on the Born approximation will fill in the Born diffraction zero, thus increasing σ_u and consequently decreasing A. By comparing with Fig. 5, we see that the Born diffraction dip in σ_u at around 30° is almost entirely filled in by partial-wave calculations. The dashed curve in Fig. 7(b) represents crudely this effect. At $\theta = 33°$, σ_u appears to be increased from its BA (Born-approximation) value by about a factor 3. (We make the comparison only crudely, since the whole DWBA curve is shifted somewhat from the BA result.) We expect that the DWBA values of A should be reduced from the BA result at this angle by about this same factor, and should thus be about 6 or 7%. This is in fact the value that we obtain. Greenstein[6] attempted to include distortion effects by using the Schiff-Tiemann approximation.[7] From
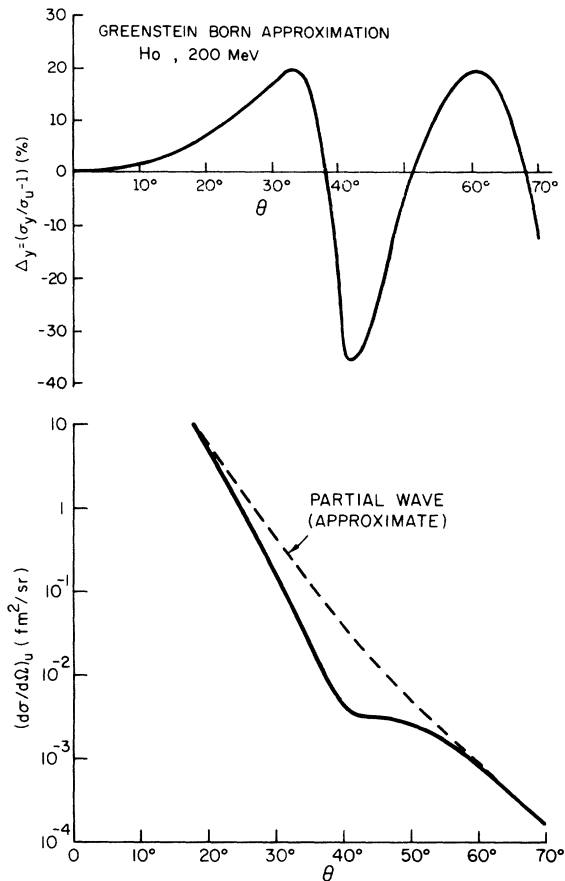
FIG. 7. The Born-approximation results of Greenstein (Ref. 6). (a) Orientation effect, Y direction, 200 MeV electrons. (b) Unoriented differential cross section (full curve) with an estimate of the partial-wave result (see Sec. VII).

Fig. 1 of Ref. 6, it appears that this approximation does not fill in the Born zero, and from Fig. 3 of Stan-Y,[1] it appears even to increase A in this range. One may conclude that, while the Schiff-Tiemann approximation has the attractive feature of including some distortion effects analytically, its linear-trajectory assumption omits just the parts of the distortion that fill in the Born zero. Its results for A are thus misleading. Penner's BA calculation,[4] with a nuclear model very similar to Greenstein's produces values for A that are considerably smaller, in fact smaller than those observed experimentally. We believe, however, that in the development of the calculation, a factor of $2I + 1 = 5$ has been omitted from Penner's $F_2(q)$. This may be seen by comparing his Eqs. (20) and (21) with our Eqs. (30) and (31). If his results are multiplied by 5, they are in reasonable agreement with Greenstein's at around 30°.

VIII. SENSITIVITY TO CHARGE SHAPE

Since the analyses of Wright and Onley predate recent experiments on deformed nuclei in the region near holmium, it is interesting to see if small but allowable changes in the nuclear model have any appreciable effect. The ZENITH method of the previous section, which we shall henceforth call DWBA, is now applied to the nuclear model whose parameters are given in the third row of Table II. This model has intrinsic radii and surface thickness compatible with recent measurements on $_{62}^{152}$Sm,[17] a quadrupole moment in agreement with Coulomb excitation experiments,[15] and its $\rho_0(r)$ and $\rho_2(r)$ are obtained by numerical inversion of Eq. (10). The alignment parameter A_2 is taken to be 0.45, the value quoted by Stan-Y.[1] The ZENITH DWBA cross section σ_u and alignment effect Δ_y are shown in Fig. 8, and Δ_y is compared with *our* result for Wright's model. The differences are significant, but quite small, considering the very appreciable changes in the multipole charge densities shown earlier in Fig. 3. While our experience is too limited to give much insight into the general shape dependence of Δ_y, two features seem fairly clear: the first maximum is dominated by the quadrupole moment; and the shape dependence becomes more pronounced at larger angles, i.e., at larger recoil momenta. The latter point will be important in obtaining a better fit to the data at the large angles.

We have concentrated on the Stan-Y data, i.e., orientation in the Y direction, for computational simplicity: partial-wave programs such as ZENITH spend most of their time computing phase shifts or channel matrices which depend only on the energy, so that the angular dependence at one energy (Stan-Y) requires very much less computation than the energy dependence at one angle (Stan-q). The approximate dependence of form factors, or cross-section ratios such as Δ, on the effective recoil wave number q_{eff}, [Eq. (18)], rather than on energy or angle separately, permits us to avoid such a huge calculation for our present purposes. Shown in Fig. 9 are curves of Δ_q obtained at three energies, $E = 150$, 200, and 300 MeV, plotted against q_{eff}. The quantity $(4/3)Ze^2/c$ appearing in Eq. (18) has the value 21.7 MeV for the model we use, the fully deformed shape whose parameter values are given in the third row of Table II. Circled on these curves are the three points which correspond to the actual experimental situation of scattering at 36°. The noteworthy feature of the three curves is that they differ very little from each other over the range of q we illustrate. This is not really surprising; the departure from q_{eff} dependence tends to occur at very large scattering
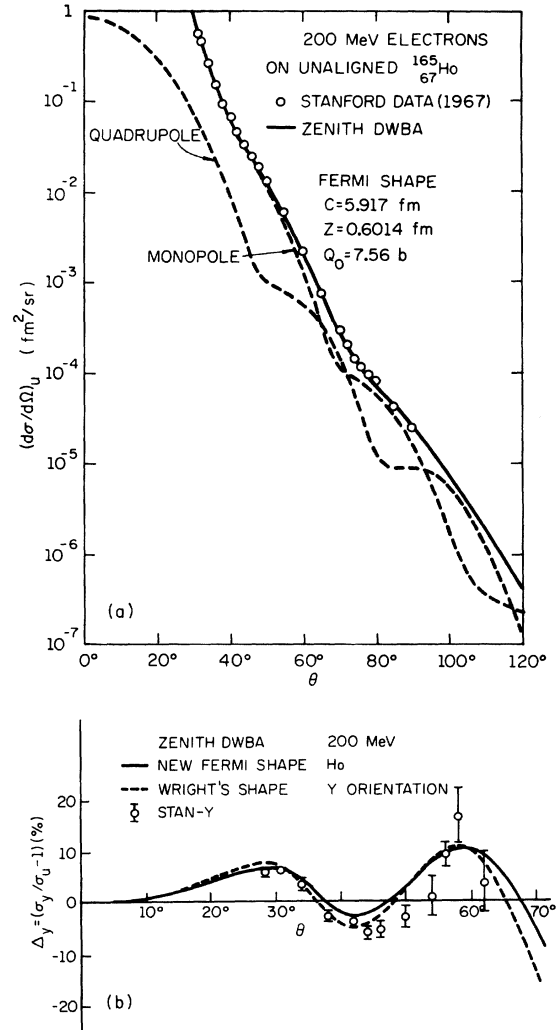
FIG. 8. 200 MeV electrons on holmium, using modified charge-distribution parameters (third row of Table II). The data is Stan-Y (Ref. 1), the curves are DWBA-like results of our coupled-channel calculations according to Sec. VII. (a) Differential cross section on unoriented nuclei, with also the monopole and quadrupole components. (b) Orientation effect, Y direction. The dashed curve is the shape used by Wright (Ref. 8), calculated by us.

angles, and the angles involved in Fig. 9 are not very large. The region $q_{eff} \lesssim 0.7$ fm^{-1} is clearly well determined by our calculations. It is also, unfortunately, significantly removed from the experimental values of Stan-q^2 which are also shown on the figure. The fact that at $\theta \sim 30°$ our model curves show a value of $\Delta_y : \Delta_q$ somewhat less in magnitude than the $-1:2$ ratio discussed in Sec. IV, while the experimental value is somewhat greater in magnitude than $-1:2$, accentuates the difference. (Wright's curves, shown in Fig.
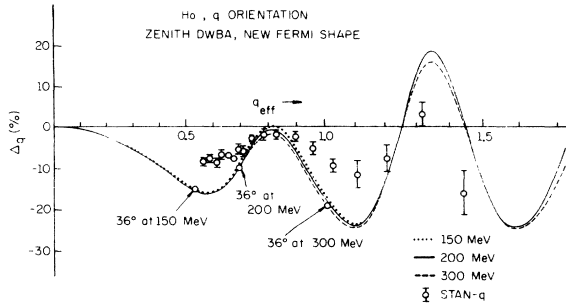
FIG. 9. Orientation effect for electrons of 150, 200, and 300 MeV on holmium nuclei oriented in the q direction. Curves come from DWBA-like calculations with the coupled-channel program. The charge-distribution parameters are from the third row of Table II. The data is Stan-q (Ref. 2).

1, display the same feature.) These results, and the physical arguments of Sec. IV, suggest that it will be very difficult to fit simultaneously both Stan-Y and Stan-q.

IX. COMPLETE ZENITH CALCULATION

The first few states of physical ^{165}Ho, and the possible monopole and quadrupole couplings among them, are shown diagrammatically in Fig. 2(b). We now present a ZENITH calculation which includes all of these couplings, for three nuclear states with the proper spin values. The number of coupled Dirac equations, $N_e \leq \sum_n (2I_n + 1)$, is 30. This is twice as big as ZENITH's previous biggest run, the three-state run in ^{152}Sm,[23] where $N_e \leq 15$. The computational effort in the coupled-channel scheme increases even more rapidly than N_e^2, so this run tests ZENITH at a new level of severity. To minimize the computation in nonessential features, and partly for reason of necessity, the following simplifications, also a feature of the other ZENITH calculations reported in this paper, are made. Electron mass and nuclear excitation energies are made equal to zero. These approximations were discussed in Ref. 22, for a very similar nucleus, and found to be adequately accurate. Only Coulomb multipole potentials are included. For this particular nucleus and these particular data (energies greater than 160 MeV and angles less than 70°) neglect of electric and magnetic multipole effects needs no further justification. For computational parameters we used the following values: the interval in kr in integrating the coupled radial Dirac equation was 0.02 out to a radius $kR_{max} = 16$; relative accuracy of the asymptotic series evaluation, and thus of the partial-wave amplitudes, was better than 1×10^{-8}. The maximum value of F, the total angular momentum,

was 36. The computation, performed in 30 min sections on an IBM 360-91 computer, took $2\frac{1}{2}$ h. In the superposition of amplitudes to construct the oriented cross section σ_0, we include both $\sigma_2^{I-I'}$ and $\sigma_4^{I-I'}$, so that all appreciable effects due to the quadrupole couplings shown in Fig. 2(b) are contained. We show the resulting orientation effect Δ in Fig. 10, compared with the DWBA results of the last section. Numerical values are given in Table IV. We observe that in Δ_y, and to a lesser extent Δ_q, there is a small difference between the complete calculation and DWBA which increases with angle. The effect is not enough to influence any comparisons with experiment that we have made previously. In particular it does not change the $\Delta_y : \Delta_q$ ratio around 30°. It is large enough compared with the experimental errors, however, that a detailed analysis will require its inclusion. It represents the dispersive corrections to the alignment effect Δ arising from these low-lying nuclear levels.

X. DISCUSSION

The effects contained in the treatment of Sec. IX are not negligible, but the improvement they make to DWBA is quite small compared with the experimental uncertainty. While any further discussion concerning a fit of the nuclear model to the data must include them, they need not affect the qualitative remarks we can make on the basis of our present results, which have not been adjusted to the data. Figures 8(a) and 8(b) show reasonable agreement between the Stan-Y experiment[1] and a reasonable nuclear model. There is thus no longer the large discrepancy between theory and experiment that appeared in Ref. 8. It is clear from Fig. 9, however, that the reasonable nuclear model is still a considerable distance from the experiment Stan-q.[2] We recall the $-1:2$ ratio that $\Delta_y : \Delta_q$ is
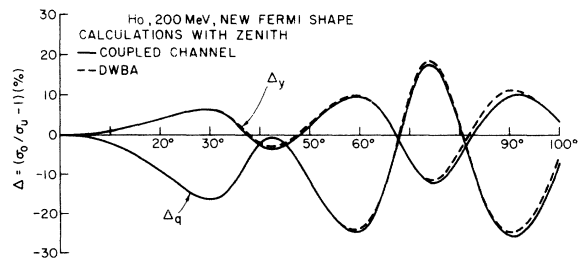
FIG. 10. Orientation effect for 200 MeV electrons on holmium nuclei oriented in the Y and the q directions using the nuclear parameters contained in the third row of Table III. The full curve is the result of the coupled-channel calculation of Sec. IX, and the dashed curve is the DWBA calculation of Sec. VIII.

expected to bear at low q, according to the estimate of Sec. IV, because of the quadrupole nature of the nuclear deformation. The calculations of Secs. VII, VIII, and IX which successively improve on that estimate to include other effects relevant to the model and the low-lying nuclear states, also exhibit this ratio. The fact that the experimental values of $\Delta_y : \Delta_q$ depart considerably from it is thus very difficult to reconcile with well-established nuclear properties. A final *theoretical* conclusion must await our anticipated detailed fit to the data, with inclusion of charge multipoles higher than quadrupole. It would be very helpful, however, if the authors of Ref. 2 could reconsider the overall magnitude of their reported Δ_q. The rest of the discussion will be concerned only with Stan-Y,[1] under the assumption that the low-q behavior of Δ is understood.

It is clear from Sec. VIII, especially from Fig. 8b, that the detailed angle dependence of Δ_y beyond its first maximum may be modified appreciably by changes in the nuclear shape. From the viewpoint of the rotational model, however, the added flexibility of the parameters associated with higher-multiple deformations requires more information than σ_u and the Δ for one orientation direction can provide. A possible source of this information is the energy-resolved scattering from the neighboring nucleus $^{166}_{68}\text{Er}$ described in Ref. 16. The nuclear model fitted to erbium is more complicated than the one we have used, indicating a somewhat different shape from that of Sec. III. A mutual fit to the holmium and erbium experiments is in progress.

A limitation on the information presently available is imposed by the necessarily rather restricted range of q covered by both the NBS[16] and Stan-Y[1] experiments. In anticipation of high-resolution experiments, perhaps with oriented nuclei, at the new higher-energy accelerators, we show in Fig. 11 the *energy-resolved* cross sections expected for *unoriented* holmium at 200 MeV. (The model parameters are those in the third row of Table II.) Shown in Fig. 12 are the orientation effects predicted for this model, for *resolved* holmium *oriented* in the Y direction. (The alignment degree A_2 is taken as 45%.) For the inelastic transitions Δ is large, fairly constant, but of opposite sign for the two transitions. It is also to be noted that the higher-order effects of our coupled-channel calculations are relatively somewhat larger than for the unresolved case. Our limited experience does not yet allow us to mark the especially significant or model-dependent features of these results, but we shall work on the problem.

We observe for future experiments that the orientation effect Δ_q is both difficult to measure (the
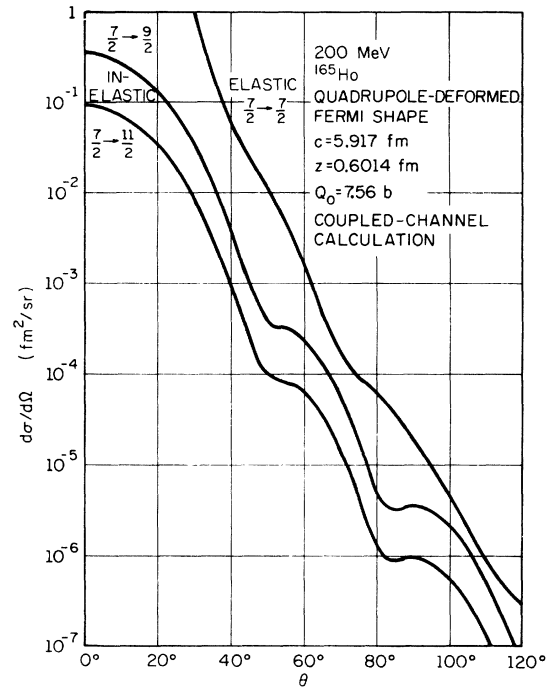
FIG. 11. Differential cross sections for energy-resolved scattering of 200 MeV electrons from unoriented holmium calculated by the coupled-channel scheme described in Sec. IX.

fixed-angle variable-energy requirement introducing perhaps unsuspected energy-dependent corrections) and a trial to analyze (partial-wave programs work at fixed energy). Measurement of Δ_x, corresponding to orientation in the scattering plane, perpendicular to the beam axis, achieves almost the same effect as Δ_q, for small scattering angles. The expected behavior of Δ_x is indicated, for the resolved elastic scattering, in Fig. 13. While on the basis of the estimate of Sec. IV the q direction, the long axis of the deformed nucleus, provides conceptually the simplest physical situation, the effects to be discovered in it are contained to a different degree in Δ_x, or in some similar orientation. Any fixed angle is trivial to calculate for. In any case, the presence of higher multipole moments in the deformation strongly suggests that more than just two orientations should be explored.

We acknowledge helpful conversations with colleagues, especially P. Axel and L. S. Cardman. The development of the estimate of Sec. IV owes much to discussions with R. L. Schult.

APPENDIX A: POPULATION MOMENTS

An equivalent and revealing way[14] to describe the nuclear orientation is in terms of the moments
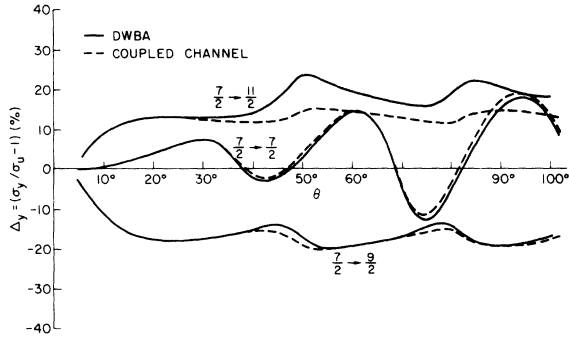
FIG. 12. Orientation effects for energy-resolved scattering of 200 MeV electrons by holmium nuclei oriented in the Y direction. The full curve is the result of the coupled-channel calculation of Sec. IX, the dashed curve from the DWBA method of Sec. VIII.

R_τ of the populations P_M with respect to the orthonormal polynomials $(-1)^{I-M}\langle IMI-M|R0\rangle$. (Here $\langle j_1m_1j_2m_2|JM\rangle$ is the angular momentum Clebsch-Gordan coefficient as defined in Ref. 20.) Thus

$$P_M = \sum_\tau R_\tau (-1)^{I-M}\langle IMI-M|\tau 0\rangle ,$$

$$R_\tau = \sum_M P_M (-1)^{I-M}\langle IMI-M|\tau 0\rangle . \tag{A1}$$

Associated with the population moments are the corresponding moments $\sigma_\tau(I \to I')$ of the oriented cross sections

$$\sigma_\tau(I \to I') = \sum_{MM'} (-1)^{I-M}\langle IMI-M|\tau 0\rangle \sigma(IM \to I'M')$$

$$\tag{A2}$$

which possess convenient spherical-tensor properties. Moments of the relative orientation effect Δ_τ may then be defined by

$$\Delta_\tau = \sum_{I'} \sigma_\tau(I \to I')/\sigma_u - 1 \tag{A3a}$$
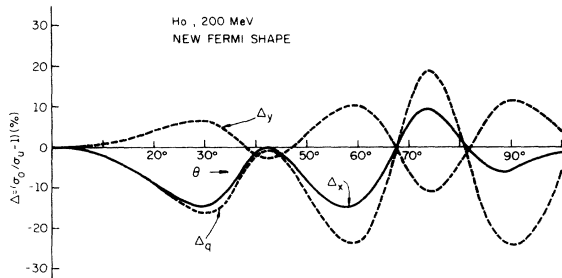
FIG. 13. Dependence of orientation effect on orientation direction for 200 MeV electrons on holmium. The three directions are X, in the scattering plane perpendicular to the beam direction; Y, the normal to the scattering plane; and q, the recoil-momentum direction.

and the experimental orientation effect Δ is given by

$$\Delta = \sum_\tau R_\tau \Delta_\tau . \tag{A3b}$$

The explicit form for A_2, the degree of alignment quoted in Refs. 1 and 2, is then

$$A_2 = \sum_M P_M[3M^2 - I(I+1)]/[I(2I-1)\sum_M P_M] . \tag{A4}$$

APPENDIX B: COUPLED-CHANNEL METHOD

The complete equations and methods used by the coupled-channel program ZENITH are presented elsewhere.[11] A simplified set of equations adequate for the present calculation is given here. We consider the scattering of an electron of negligible rest mass from an infinitely massive nucleus characterized by a finite number N of degenerate-energy eigenstates $|nM\rangle$, each an eigenstate of spin I_n, z component of spin M, and parity p_n, where $1 \le n \le N$. Eigenstates of the orbital angular momentum and spin of the electron, $|LM_L\rangle$ and $|\frac{1}{2}M_s\rangle$, are combined into eigenstates of the total angular momentum of the electron in the usual manner[20]:

$$|JL\mu\rangle = \sum_{m_s M_L} \langle LM_L\tfrac{1}{2}m_s|J\mu\rangle|LM_L\rangle|\tfrac{1}{2}m_s\rangle .$$

The phases of the various kets are chosen so that under time reversal $T|LM_L\rangle = (-1)^{L+M_L}|L-M_L\rangle$, etc. Thus $\langle \theta\varphi|LM_L\rangle = i^L Y(\theta\varphi)$. J and the two possible corresponding values of L may be combined into a single quantum number χ such that

$$J = |\chi| - \tfrac{1}{2} ,$$

$$L = J + \tfrac{1}{2}\,\mathrm{sgn}\chi .$$

For a given total energy E, the wave function of the scattering system satisfies the wave equation

$$[-i\vec{\alpha}\cdot\vec{\nabla} + e\varphi(\vec{r})]\Psi(\vec{r}) = E\Psi(\vec{r}),\quad \vec{\alpha} = \begin{pmatrix} 0 & \vec{\sigma} \\ \vec{\sigma} & 0 \end{pmatrix}, \tag{B1}$$

where $\varphi(\vec{r})$ is the Coulomb field of the nucleus, the only electromagnetic interaction needed here. With $\vec{F} = \vec{I} + \vec{J}$ the total angular momentum, we wish to expand $\Psi(\vec{r})$ in eigenfunctions of $\vec{F}^2$, F_3, and P, the total parity operator for the system. One such set of eigenfunctions is

$$|fm_f p\chi n\rangle = \sum_{\mu M} \langle J\mu I_n M|fm_f\rangle|\chi\mu\rangle|nM\rangle$$

for which $p = p_n(-1)^L$. In general, to a pair of eigenvalues f and p, there correspond several pos-

sible pairs (χ, n). Let $\mathfrak{N}(f,p)$ be the set of such pairs, and let $N(f,p)$ be its cardinality. It is clear that if $(\chi, n) \in \mathfrak{N}(f,p)$ then $(-\chi, n) \in \mathfrak{N}(f,p)$. As a notational convenience, we introduce a single quantum number j, such that as j ranges from 1 to $N(f,p)$, (χ_j, n_j) ranges over all of the pairs in $\mathfrak{N}(f,p)$. Finally, if j is the quantum number corresponding to the pair (χ, n) in $\mathfrak{N}(f,p)$, let j_- be that corresponding to the pair $(-\chi, n)$ in $\mathfrak{N}(f, -p)$. We may now expand the total wave function as

$$\Psi(\vec{r}) = \sum_{\substack{fm_fp \\ ij}} \alpha^i_{fm_fp} \frac{1}{r} \begin{pmatrix} g^{ij}_{fp}(r) |fm_fpj\rangle \\ -\text{sgn}\chi_j f^{ij}_{fp}(r) |fm_f -pj_-\rangle \end{pmatrix}, \quad \text{(B2)}$$

where the coefficients $\alpha^i_{fm_fp}$ are constants which must be chosen to satisfy the scattering boundary condition. Substituting this expression into Eq.

(B1) we obtain, in terms of the dimensionless radial variable $\rho = rE$, the differential equations

$$\left(\frac{d}{d\rho} - \frac{\chi_j}{\rho}\right) f^{ij}_{fp}(\rho) + g^{ij}_{fp}(\rho) = \sum_{j'} S^f_{jj'}(\rho) g^{ij'}_{fp}(\rho) ,$$

$$\left(\frac{d}{d\rho} + \frac{\chi_j}{\rho}\right) g^{ij}_{fp}(\rho) - f^{ij}_{fp}(\rho)$$

$$\text{(B3)}$$

$$= -\sum_{j'} \text{sgn}(\chi_j \cdot \chi_{j'}) S^f_{j_-j'_-}(\rho) f^{ij'}_{fp}(\rho) ,$$

in which

$$S^f_{jj'}(\rho) = \langle fm_fpj | \frac{e\varphi(\vec{r})}{E} | fm_fpj'\rangle .$$

The matrix element $\langle nM | \varphi(\vec{r}) | n'M'\rangle$ may be expanded in spherical harmonics, in the form

$$\langle nM | \varphi(\vec{r}) | n'M'\rangle = \sum_{lm} (-1)^m \langle I'M'l - m | IM\rangle \frac{i^l}{(2I+1)^{1/2}} \varphi^{nn'}_l(r) Y_{lm}(\theta\varphi) .$$

The coupling potential $S^f_{jj'}(\rho)$ may now be expressed in terms of the multipole potentials $\varphi^{nn'}_l(r)$:

$$S^f_{jj'}(\rho) = (e/E)(-1)^{f+I-1/2}[(2L+1)(2J+1)(2J'+1)]^{1/2}$$

$$\times \sum_l (-1)^{(L'+L+1)/2} \langle L0l0 | L'0\rangle \begin{Bmatrix} J & J' & l \\ L' & L & \frac{1}{2} \end{Bmatrix} \begin{Bmatrix} J & J' & l \\ I' & I & f \end{Bmatrix} [(2l+1)/4\pi]^{1/2} \varphi^{nn'}_l(r) . \quad \text{(B4)}$$

It follows from time reversal invariance that

$$S^f_{jj'}(\rho) = \text{sgn}(\chi\chi') S^f_{j_-j'_-}(\rho) .$$

The superscript i on the functions f and g above distinguishes among the $N(f,p)$ solutions of Eqs. (B3) which are regular at the origin, according to their particular behavior at the origin, as follows:

$$\lim_{\rho \to 0} [f^{ij}_{fp}(\rho)\rho^{-\chi_j}] = \delta_{ij}, \quad \lim_{\rho \to 0} [g^{ij}_{fp}(\rho)\rho^{-\chi_j}] = 0,$$

$$\chi_j > 0;$$

$$\lim_{\rho \to 0} [f^{ij}_{fp}(\rho)\rho^{\chi_j}] = 0, \quad \lim_{\rho \to 0} [g^{ij}_{fp}(\rho)\rho^{\chi_j}] = \delta_{ij},$$

$$\chi_j < 0 .$$

The major part of any coupled-channel scheme is the numerical integration of Eqs. (B3) from the origin out to some large radius, where they may be compared with standard solutions. In ZENITH, these standard solutions are defined by asympototic expansions of the asymptotic forms of Eqs. (B3), including all multipole potentials $S^f_{jj'}(\rho)$. The analytic and computational details are described in Ref. 11 and will not be gone into here. By such a method, it is possible to determine completely the asymptotic behavior of f^{ij}, g^{ij} in

the form

$$g^{ij}_{fp}(\rho) \sim A^{ij}_{fp} \sin(\rho + \gamma \ln 2\rho - L_j\pi/2 + \delta^{ij}_{fp}) ,$$

$$f^{ij}_{fp}(\rho) \sim A^{ij}_{fp} \cos(\rho + \gamma \ln 2\rho - L_j\pi/2 + \delta^{ij}_{fp}) ,$$

where $\gamma = Ze^2$. We refer to the (numerically determined) quantities A^{ij}_{fp} and δ^{ij}_{fp} as the amplitudes and phase shifts, respectively, of the (f,p) partial wave. Considered as an $N(f,p)$ by $N(f,p)$ matrix, $A^{ij}_{fp} \exp(-i\delta^{ij}_{fp})$ has an inverse which we denote by h^{ij}_{fp}.

The constants $\alpha^i_{fm_fp}$ may be chosen so that the spherically incoming portion of $\Psi(\vec{r})$ is asymptotically equal to the spherically incoming portion of a plane wave approaching the electron from the negative z axis. For definiteness, we suppose that initially the nucleus is in its ground state $|1M\rangle$ and the electron spin has projection m_s on the z axis. Then

$$\alpha^i_{fm_fp} = \sum_j [2\pi(2L_j+1)]^{1/2} h^{ij}_{fp} \langle J_j m_s I_j M | fm_f\rangle$$

$$\times \langle L_j 0 \tfrac{1}{2} m_s | J_j m_s\rangle \delta_{1n_j} .$$

The scattering amplitudes $f^{m_s^M M_s^M I^M_s}_{1-r}(\theta\varphi)$ are defined in terms of the asymptotic behavior of $\Psi(\vec{r})$ by the equation

$$\Psi(\vec{r}) \sim e^{ix} \left| \tfrac{1}{2} m_s \right\rangle \left| 1 M \right\rangle$$

$$+ (e^{i\rho}/\rho) \sum_{rM_I M_s} f^{m_s M M_I M_s}_{1 \to r}(\theta\varphi) \left| \tfrac{1}{2} M_s \right\rangle \left| r M_I \right\rangle .$$

(B5)

In Eq. (B5) the logarithmic terms have been omitted from the exponents and only the upper components of $\Psi(\vec{r})$ have been included. In terms of the partial-wave phase shifts and amplitudes

$$f^{m_s M M_I M_s}_{1 \to r}(\theta\varphi) = \sum_{fpjk} M^{jk}_{fpr}(2L_j + 1)^{1/2} \langle J_j m_s I_1 M | fm_f \rangle$$

$$\times \langle L_j 0 \tfrac{1}{2} m_s | J_j m_s \rangle \langle J_k M_J I_r M_I | fm_f \rangle$$

$$\times \langle L_k M_L \tfrac{1}{2} M_s | J_k M_J \rangle Y_{L_k M_L}(\theta\varphi) ,$$

where $M_L = m_s + M - M_I - M_s$ and

$$M^{jk}_{fpr} = -\sum_{\bar{i}} i \sqrt{\pi}\, h^{ij}_{fp} A^{ij}_{fp} e^{i\delta^{ij}_{fp}} \delta_{1n_j} \delta_{r n_k} .$$

Note that although the partial-wave phase shifts and amplitudes depend upon the particular set of regular solutions of Eqs. (B3) that is chosen, M^{jk}_{fpr} and, hence, $f^{m_s M M_I M_s}_{1 \to r}(\theta\varphi)$ do not. The scattering amplitudes have the following symmetries:

$$f^{-m_s -M -M_I -M_s}_{1 \to r}(\theta, -\varphi)$$

$$= p_r p_1 (-1)^{I_0 - I_r - M_L} f^{m_s M M_I M_s}_{1 \to r}(\theta, \varphi) \quad \text{(B6a)}$$

which reflects parity conservation and

$$f^{1/2 M M_I -1/2}_{1 \to r}(\theta, \varphi) = \tan\tfrac{1}{2}\theta e^{i\varphi} f^{1/2 M M_I 1/2}_{1 \to r}(\theta, \varphi) \quad \text{(B6b)}$$

which represents helicity conservation, a consequence of neglecting the mass of the electron.

[1] R. S. Safrata, J. S. McCarthy, W. A. Little, M. R. Yearian, and R. Hofstadter, Phys. Rev. Lett. 18, 667 (1967), which we refer to as Stan-Y.

[2] F. J. Uhrhane, J. S. McCarthy, and M. R. Yearian, Phys. Rev. Lett. 26, 578 (1971), which we refer to as Stan-q.

[3] H. Überall, *Electron Scattering from Complex Nuclei* (Academic, New York, 1971), Part A, Secs. 4.4 and 5.3.

[4] S. Penner, National Bureau of Standards internal report, 1960 (unpublished).

[5] L. E. Wright and D. S. Onley, Nucl. Phys. 64, 231 (1965).

[6] H. B. Greenstein, Phys. Rev. 144, 902 (1966).

[7] The Schiff-Tiemann approximation [L. I. Schiff, Phys. Rev. 103, 443 (1956); J. J. Tiemann, *ibid.* 109, 183 (1958)]. This approximation uses an eikonal approach, but with linear trajectories.

[8] L. E. Wright, Nucl. Phys. A135, 139 (1969), which we refer to as W1.

[9] L. E. Wright, reported as a private communication in Ref. 2. We refer to it as W2.

[10] We thank J. Heisenberg for pointing out the desirability of a further examination of this problem.

[11] R. L. Mercer, Ph.D. thesis, Department of Computer Science, University of Illinois, 1972 (unpublished); R. L. Mercer (unpublished).

[12] If the external magnetic field were not strong enough to saturate the spins, then a possible helical spin pattern could result. This would have the effect of a nutation of the spin direction of neighboring nuclei, which would decrease the effective alignment. As will be seen later, we have had no need to invoke this effect. We thank Professor M. B. Salamon and Professor C. P. Slichter for helpful conversations on this point.

[13] We thank Professor W. A. Little for a helpful conversa-

tion on this point.

[14] This is the method of statistical tensors, U. Fano, National Bureau of Standards Report No. 1214, 1951 (unpublished). It is used somewhat obscurely in Ref. 6, and is also described in Ref. 3, p. 260.

[15] A. Buryn, Nucl. Data Sheets 11, 189 (1974). See adopted value, p. 231.

[16] T. J. Cooper, Ph.D. thesis, Massachusetts Institute of Technology, 1974 (unpublished), quotes $\beta_{4c} = 0.0199$ for $^{166}_{68}$Er, a neighboring nucleus.

[17] W. Bertozzi, T. Cooper, N. Ensslin, J. Heisenberg, S. Kowalski, M. Mills, W. Turchinetz, C. Williamson, S. P. Fivozinsky, J. W. Lightbody, Jr., and S. Penner, Phys. Rev. Lett. 28, 1711 (1972).

[18] We chose the $^{152}_{62}$Sm parameters, rather than those for ^{166}Er from Ref. 16, since samarium appears to be well explained by the model we have assumed, whereas erbium is more complex. We hope to pursue at a later date the inclusion in the holmium analysis of the interesting information on erbium contained in Ref. 16.

[19] A. Bohr and B. R. Mottelson, K. Dan. Vidensk. Selsk., Mat.–Fys. Medd. 27, 16 (1953).

[20] For angular momentum functions, we use the standard phase conventions as defined for example, in K. Gottfried, *Quantum Mechanics* (Benjamin, New York, 1966), Vol. I. The quantity $\langle j_1 m_1 j_2 m_2 | JM \rangle$ is the Clebsch-Gordan coefficient, Sec. 25. The six-j symbol

$$\begin{Bmatrix} j_1 & j_2 & j_3 \\ j_4 & j_5 & j_6 \end{Bmatrix}$$

is defined in Sec. 36.4. The rotation matrices $D^{(j)}_{mm'}(\alpha\beta\gamma)$ are defined in Sec. 34.4.

[21] L. I. Schiff, Phys. Rev. 96, 765 (1954).

[22] See, for example, S. Moszkowski, *Handbuch der Physik*, edited by S. Flügge, (Springer, Berlin, 1957), Vol. 39, p. 481.

[23] A brief nontechnical description of ZENITH's methods was given in R. L. Mercer and D. G. Ravenhall, Phys.

Rev. C 10, 2002 (1974).

[24]Duke program, described in S. T. Tuan, L. E. Wright, and D. S. Onley, Nucl. Instrum. Methods 60, 70 (1968), and run for us by L. S. Cardman.

[25]HEINEL, a code based on the Duke program written by J. Heisenberg, as mentioned in J. Heisenberg, I. Sick, and J. S. McCarthy, Nucl. Phys. A164, 353 (1971). A copy of this code was run for us by L. S. Cardman.